

Supporting Information to “Antibacterial, Wearable, Transparent Tannic Acid-Thioctic Acid-Phytic Acid Hydrogel for Adhesive Bandage”

**Xian-hui Shao¹; Xiao Yang²; Yue Zhou¹; Qing-chang Xia¹; Yun-ping Lu¹;
Xiao Yan¹; Chen Chen^{*1}; Ting-ting Zheng^{*1}; Lin-lin Zhang^{*1}; Yu-ning Ma¹;
Yu-ning Ma¹; Shu-zhong Gao¹**

¹Key Laboratory of New Material Research Institute, Department of Acupuncture-Moxibustion and Tuina, Shandong University of Traditional Chinese Medicine, Jinan 250355, China

²The First Affiliated Hospital of Shandong First Medical University (Shandong Qianfoshan Hospital), Jinan 250014, China

*Correspondence to: C. Chen, T. T. Zheng and L. L. Zhang (E-mail: 21129008@zju.edu.cn; ttz10_10@163.com and linlin66210@outlook.com)



Figure S1 Photos on Hydrogels that were pre-wetted and adhered onto the window.

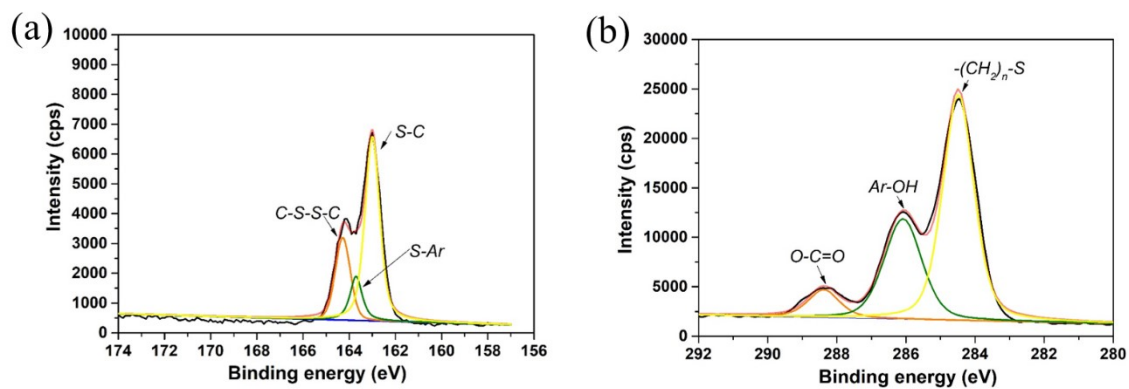


Figure S2 XPS spectra of the hydrogel. (a) S2p spectrum of TATAPA-2 hydrogel; (b) C1s spectrum of TATAPA-2 hydrogel.

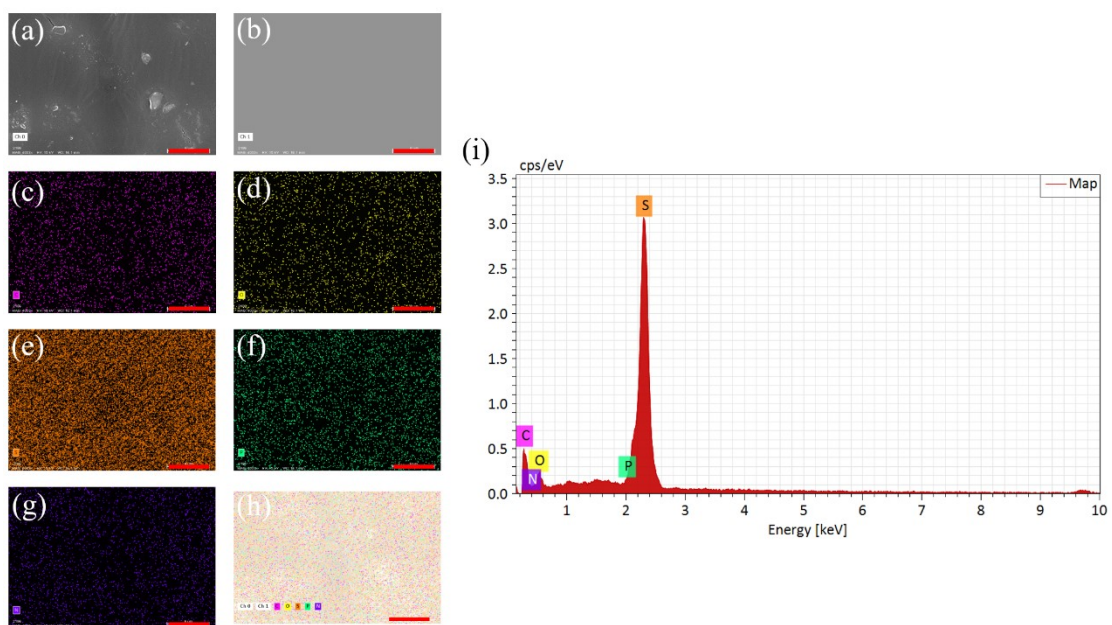


Figure S3 (a,b) The morphology of TATAPA-2 hydrogel view by SEM; (c-h) Elementary mapping images of the TATAPA-2 hydrogel; (i) Energy-dispersive spectroscopy spectrum.

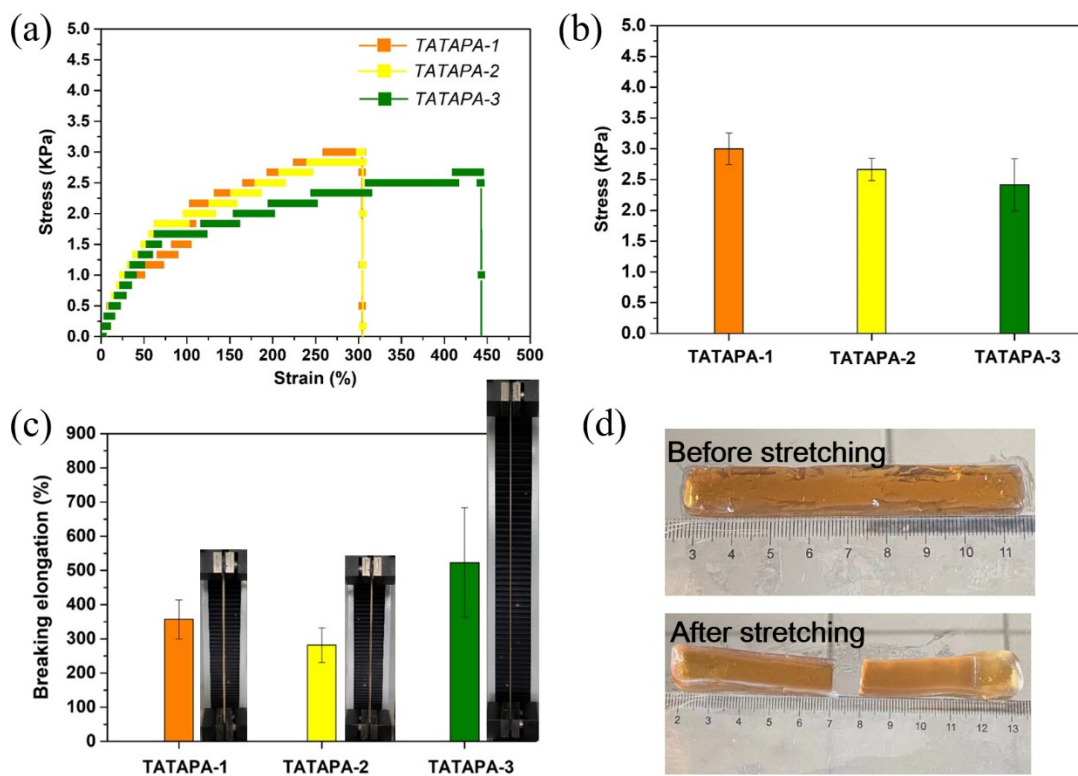


Figure S4 (a) Stress-strain curves of TATAPA-1, TATAPA-2 and TATAPA-3 hydrogels; (b) Tensile strength of the hydrogels; (c) Maximum breaking elongation of the hydrogels; (d) Photos of the TATAPA-2 hydrogel before and

after stretching.

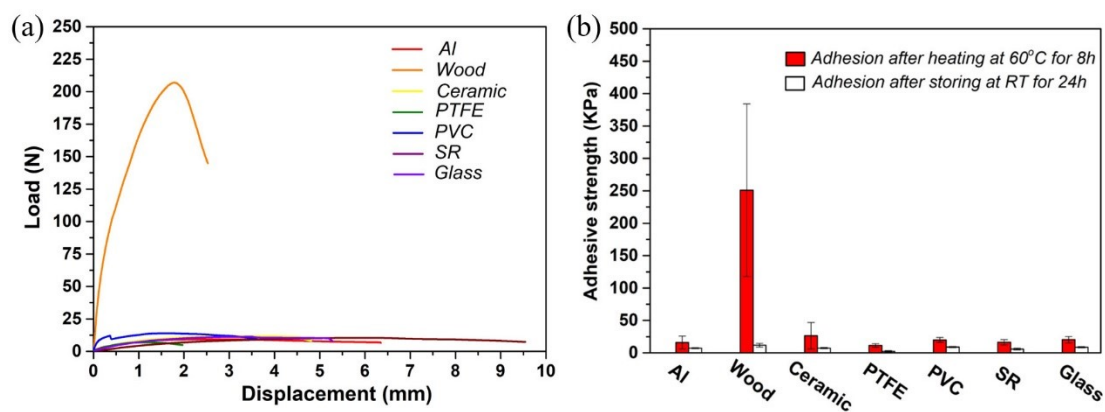


Figure S5 Adhesive properties of the dried TATAPA hydrogels. (a) Representative load-displacement curves of the TATAPA-2 patch (25 mm width, 25 mm length, 1 mm thickness) to various daily used substrates; (b) Adhesive strength of the dried TATAPA-2 hydrogel with different substrates.

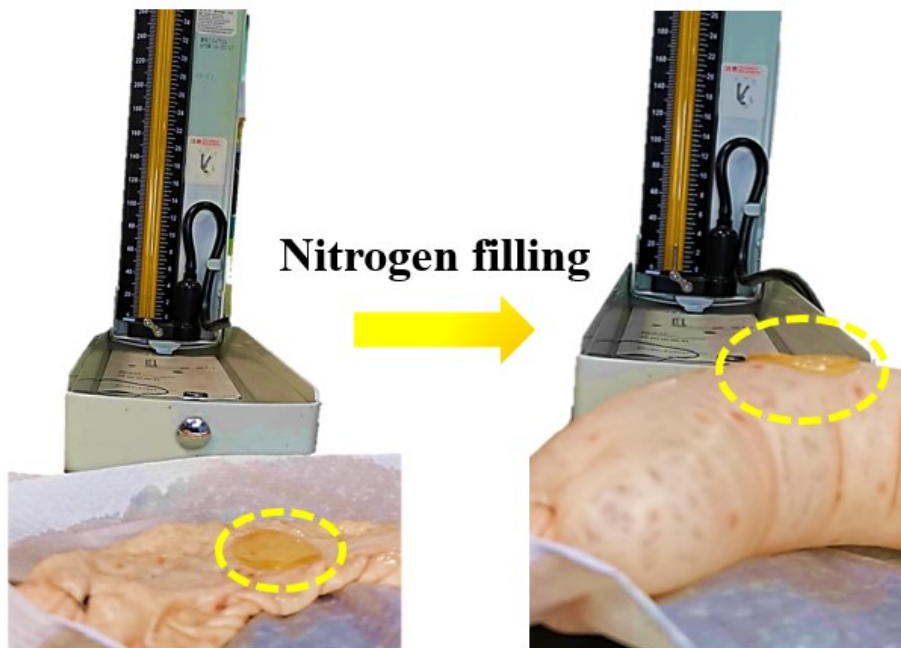


Figure S6 Images on the TATAPA-adhered intestine membrane before and after nitrogen filling

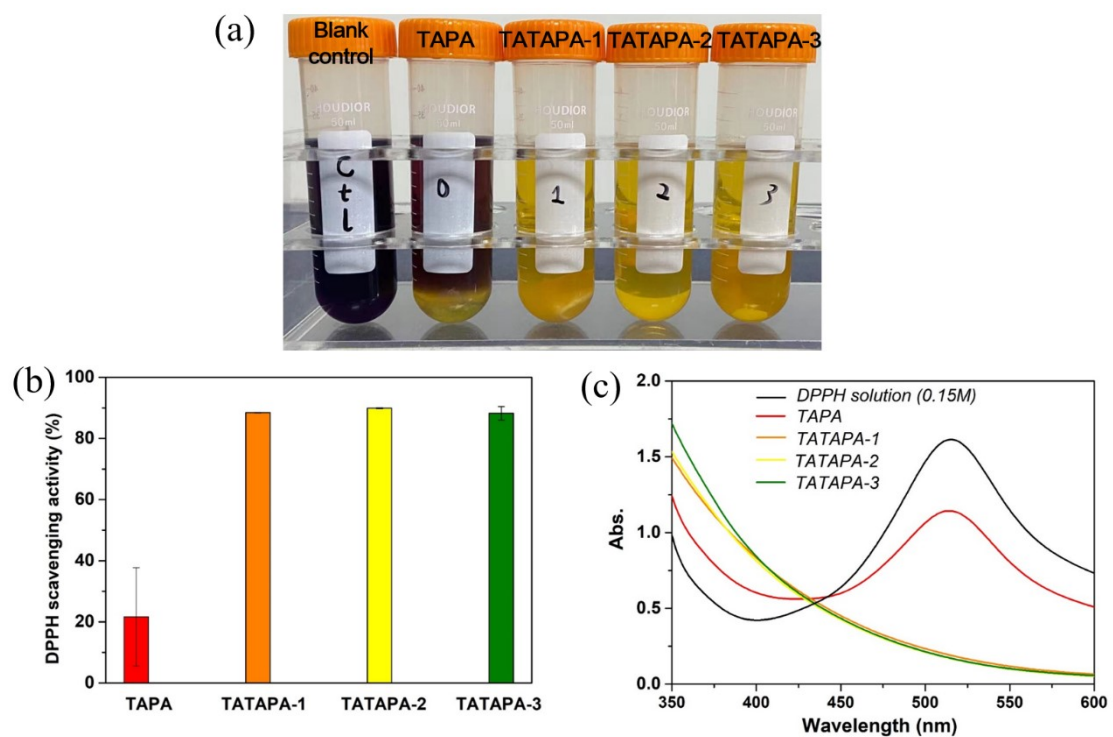


Figure S7 (a) Image of DPPH ethanol solutions (0.15 mM) after various hydrogels immersion for 10 min; (b) Antioxidant abilities of the TAPA, TATAPA-

1, TATAPA-2 and TATAPA-3 hydrogels; (c) UV-vis spectra of DPPH solutions before and after various hydrogels immersion.

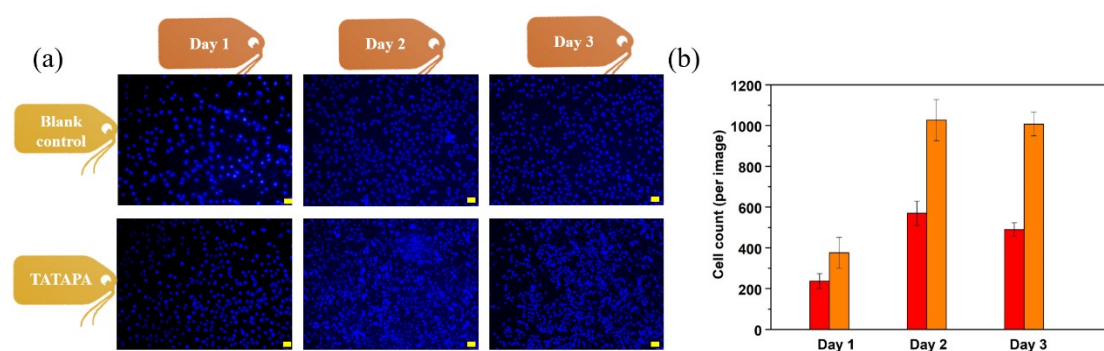


Figure S8 *In vitro* biocompatibility studies of the TATAPA-2 hydrogel with L929 cells. (a) Photos of the DAPI stained cells, scale bar=50 μm ; (b) cell count (per image) of the blank control and TATAPA-2 hydrogel in function of time.

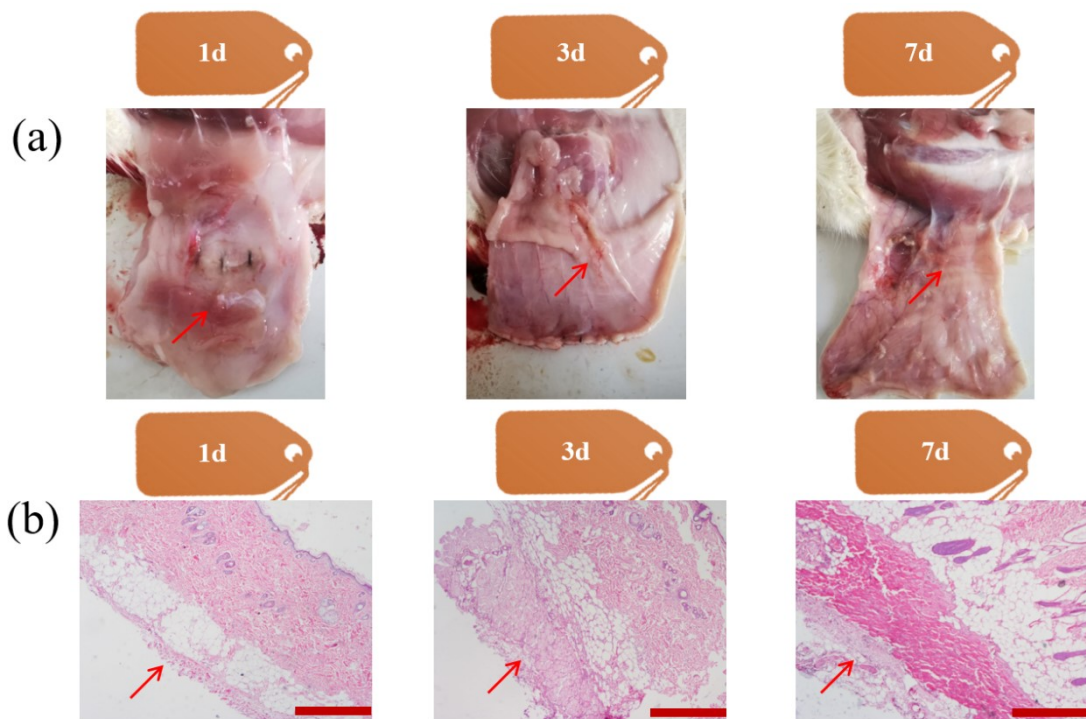


Figure S9 *In vivo* degradation of the TATAPA-2 hydrogel. (a) Photos on the degradation process of the TATAPA-2 hydrogel after implanted under the rats' skin; (b) H&E staining images of the adjacent tissue at 1d, 3d and 7d day, scale bar=500 μm .

Supporting Movies

Movie S1: Wearable TATAPA hydrogel on the arm of the corresponding author.

The movie is real-time.

Movie S2: The facile peeling off performance of TATAPA hydrogel. The movie is real-time.

Movie S3: The utilization of TATAPA hydrogel as a waterproof tape for a broken rubber waterpipe. The movie is real-time.

Movie S4: The hemostatic effect of TATAPA hydrogel in a rat femoral artery model. The movie is real-time.

Movie S5: The hemostatic effect of TATAPA hydrogel in a rat liver hemostasis model. The movie is real-time.